RSC Advances

ROYAL SOCIETY OF CHEMISTRY

www.rsc.org/advances

Mussel-inspired Ultrathin Film on Oxidized Ti-6Al-4V Surface for Enhanced BMSC's Activities and Antibacterial Capability

Ziyuan Wang[1], *Malcolm Xing*[1,2]* *and Olanrewaju Ojo*[1]*

[1]Department of Mechanical Engineering, University of Manitoba, Winnipeg, Manitoba, Canada

[2]Manitoba Institute of Child Health, Winnipeg, Manitoba, Canada

*Corresponding authors: Malcolm.xing@umanitoba.ca

Olanrewaju.Ojo@umanitoba.ca

Keywords: Mussel-inspired Dopamine; Layer-by-Layer Self-assembly; Ti-6Al-4V; Osteogenic Differentiation; Anti-bacteria.

Abstract: To improve the biocompatibility and antibacterial capability of thermally oxidized Ti-6Al-4V, an ultrathin alginate/chitosan film that contains nano-silver was constructed through mussel-inspired poly(dopamine). The hybrid structure was successfully fabricated on Ti-6Al-4V surface without deteriorating the rough surface induced by thermal oxidation (TO). The hybrid surface was characterized by the use of contact angle goniometer (CAG), atomic force microscope (AFM), scanning electron microscope (SEM), X-ray photoelectron spectrometer (XPS), and energy dispersive spectrometer (EDS). Bone marrow stem cell (BMSC) viability, morphology and proliferation tests showed that they were significantly increased by the biomimetic chitosan/alginate film on Ti-6Al-4V. Further, nano-silver particles incorporated into the chitosan/alginate film inhibited the growth of *Escherichia coli* (*E. coil*) and *Staphylococcus aureus* (*S. aureus*) without jeopardizing the improved BMSC viability, morphology and proliferation. More importantly, the expression of alkaline phosphatase (ALP) was significantly up-regulated after BMSCs was cultured on the Ti-6Al-4V-based hybrid structure. Taken together, this study presents a promising strategy to improve biocompatibility and antibacterial capability of thermally oxidized Ti-6Al-4V alloy.

■ Introduction

Various surface modification techniques have been employed to alter the surface characteristics of bio-implantable titanium and its alloys. These include traditional techniques such as thermal oxidation (TO), chemical treatment, sandblasting and recently emerged techniques like layer-by-layer (LBL) self-assembly of polyelectrolytes, nano-patterning and biomolecules immobilization, etc. [1-7]. Among traditional techniques, TO can produce a nodular surface topography that consists of nano- to micron- scale fine oxide particles [8]. Both *in vitro* and *in vivo* studies have

demonstrated that this nodular topography is advantageous in bone-implant integration [1, 9-10]. However, the bio-inert nature of thermally oxidized titanium and its alloys makes them unable to mimic the extracellular microenvironment, which is essential in regulating the implant-cell interactions [11]. Therefore, further modification of thermally oxidized titanium and its alloys is very necessary.

Besides inadequate biocompatibility, bacterial contamination also largely compromises the long-term success of implants [12]. The biofilm formed at the bone-implant interface is highly resistant to host defense and accounts for a high percentage of implant failure. One of the most promising strategies to overcome this situation is the incorporation of nano-silver into implants. It has been demonstrated that at suitable dose, nano-silver exhibits wide antibacterial spectrum, low cytotoxicity and long-term antibacterial characteristics [13].

Recently, the LBL self-assembly of polyelectrolytes has gained increasing interest. The films formed by electrostatic force attraction are ideal platforms to mimic the extracellular microenvironment [14]. Assembly of different polyelectrolytes such as chitosan/alginate, PLL/DNA and chitosan/gelatin has been carried out to regulate implant-cell interactions [15-19]. Meanwhile, the LBL film can also function as a carrier to load bone-related chemicals like fibronectin, BMP 2, etc. [20]. However, this technique has not been reported to improve the biocompatibility and antibacterial capability of thermally oxidized Ti-6Al-4V surface.

Aims to improve the biocompatibility and antibacterial capability of thermally oxidized Ti-6Al-4V, we herein fabricated an ultrathin alginate/chitosan surface film that contains nano-silver through poly(dopamine), which exhibits a comparable structure to the adhesive proteins secreted by mussels (Scheme1). In this study, we first monitored the alginate/chitosan film fabrication process and selected the optimal alginate/chitosan pair number to be constructed onto the

thermally oxidized Ti-6Al-4V surface. Then we incorporated nano-silver into the selected alginate/chitosan film and characterized the topographical properties of different samples. Finally, the *in vitro* performance of the Ti-6Al-4V-based hybrid structure was evaluated through BMSC viability, morphology, proliferation and differentiation assays.

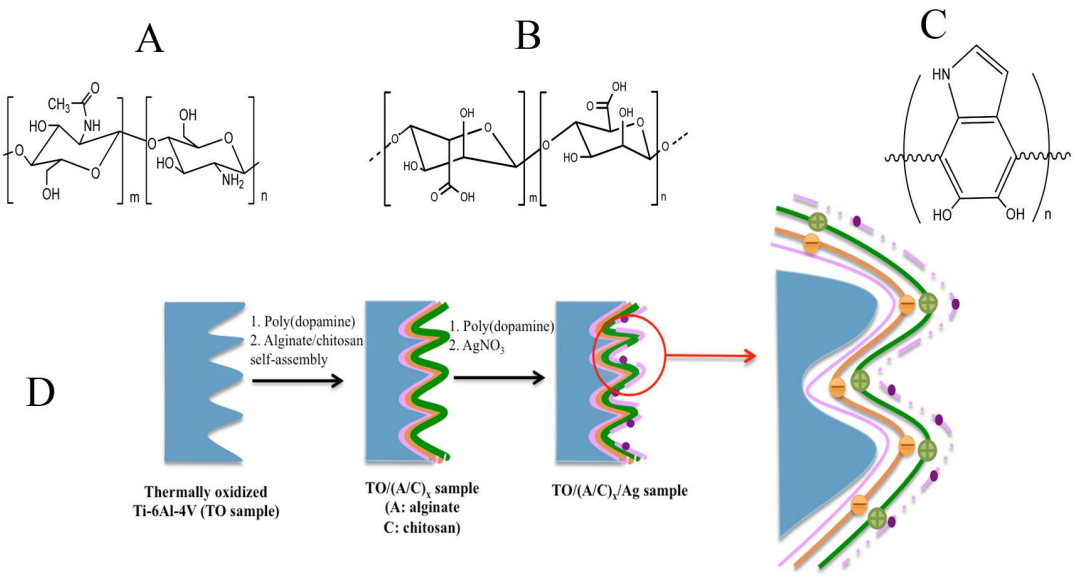

Scheme 1. The molecular structure of A) Chitosan, B) Alginate, C) Poly(dopamine) and D) the construction process of the mussel-inspired film onto thermally oxidized Ti-6Al-4V surface.

■ Materials and Methods

Materials. A Ti–6Al–4V (ASTM F-1472) round bar that was 12.7 mm in diameter was purchased from Titanium Industries, Inc. (QB, Canada). Medium molecular weight chitosan (75-85% deacetylated) and alginic acid sodium salt (viscosity of 2% solution at 25 °C ~ 250 cps) were purchased from Sigma-Aldrich Chemical Co. (MO, USA). Dopamine hydrochloride was obtained from Alfa Aesar (MA, USA). Other chemicals were purchased from Fisher Scientific (ON, Canada). Mouse BMSCs were purchased from American Type Culture Collection (MD,

USA). As received Dulbecco's modified Eagle's medium (DMEM), fetal bovine serum (FBS) and related cell culture reagents were purchased from Gibco (ON, Canada) and used without further treatment. Live/Dead® viability assay kit, TRIzol and Oligo dT were obtained from Invitrogen (CA, USA). methylthiazoltetrazolium bromide (MTT) cell proliferation assay kits were purchased from Biotium Inc. (CA, USA). All chemicals were used as-received unless otherwise specified.

Methods

Thermal Oxidation of Ti-6Al-4V alloy.

The Ti-6Al-4V bar was cut into circular shapes that were 12.7 mm in diameter and 1 mm in thickness with a numerically controlled wire electro-discharge machine. These samples were polished to 1μm to form mirror-like surfaces and ultrasonically washed for 15 mins with ethanol, acetone and ultrapure water, followed by drying using a stream of compressed air. To fabricate thermally oxidized Ti-6Al-4V, the samples were placed into a laboratory furnace under an atmospheric condition at 650°C for 8 h. After oxidation treatment, all of the samples were ultrasonically washed with ethanol, acetone and ultrapure water for 15 mins, then dried and stored under a nitrogen gas atmosphere. Thereafter, the polished and thermally oxidized Ti-6Al-4V disks were denoted as P sample and TO sample, respectively.

Preparation of Polyelectrolytes.

Poly(dopamine) (PDA) solution was prepared by dissolving dopamine into Tris-HCl buffer (0.1 mM, pH=8.5) at a concentration of 2 mg/ml. A chitosan solution (5 mg/ml), used to fabricate the positively charged layer, was obtained by dissolving chitosan into 0.1 M HCl that contained 0.14

M NaCl. An alginate solution (5mg/ml), used to fabricate the negatively charged layer, was prepared by dissolving alginic acid into 0.1 M NaOH that contained 0.14 M NaCl. After dissolution, chitosan solution was adjusted to pH=5 and alginate solution was adjusted to pH=8 by using either NaOH or HCl.

Construction of Alginate/Chitosan Film.

The TO sample was first immersed into the PDA solution overnight to obtain an adhesive precursor prior to the construction of alginate/chitosan film. Then the PDA-treated sample was placed in the vacuum chunk of a spin-coater (Headway, USA) to fabricate the alginate/chitosan film. Briefly, PDA-treated sample was pipetted with 300 µl alginate solution, followed by spinning at 2500 rpm for 90 secs. The sample was then washed twice with ultrapure water at 1000 rpm for 60 secs. Thus, a negatively charged alginate layer was obtained on the PDA-treated sample surface. The fabrication of chitosan layer was carried out by using the same procedure as alginate. Finally, this process was repeated until the desired number of alginate/chitosan pairs was attained. The resultant fabrication was denoted as TO/$(A/C)_X$ sample, where A, C and x represented alginate, chitosan and the number of alginate/chitosan pairs, respectively.

Incorporation of Nano-silver.

The TO/$(A/C)_X$ sample was immersed into the PDA solution (2 mg/ml) for 3 h in the dark and washed twice with ultrapure water. The sample was then immersed into 10 mM $AgNO_3$ solution for 3 h in the dark to reduce the silver ions into metallic nano-silver particles, subsequently rinsed three times with ultrapure water and finally dried in air. The resultant fabrication was

denoted as TO/$(A/C)_X$/Ag sample, where A, C and x represented alginate, chitosan and the number of alginate/chitosan pairs, respectively.

Characterization.

The contact angle measurements were conducted on an NRL-100-00-115-S contact angle goniometer (Rame-Hart, USA) to monitor the wettability changes during the alginate/chitosan film fabrication process. The droplets were controlled so that they were all identical in size during testing. Each sample was tested three times to ensure the repeatability of the experiment. An atomic force microscope (Vecco D3100, USA) was used to examine the surface topography and roughness of the Ti-6Al-4V samples. A surface area of 10×10 μm^2 was scanned under a tapping mode at room temperature.

A JEOL 5900 scanning electron microscope was employed to characterize the surface topographies of Ti-6Al-4V samples. Additionally, an X-ray photoelectron spectroscopy analysis was carried out with an Axis DLD Ultra X-ray photoelectron spectrometer with an Al Kα (1486.6 eV) monochromatic source at base pressures less than 10^{-8} Torr and a perpendicular take-off angle. The energy shift due to the surface charge was corrected with C 1s that had a binding energy of 285 eV.

Antibacterial Evaluation.

Gram-negative bacteria *Escherichia coli (E. coli)* and gram-positive bacteria *Staphylococcus aureus* (*S. aureus*) were used to evaluate the antibacterial capability of all the Ti-6Al-4V samples. The broth that contained *E. coli* and *S. aureus* were centrifuged at 3000 rpm for 10 mins. After the removal of the supernatant, the *E. coli* and *S. aureus* were washed twice with

phosphate-buffered saline (PBS) and re-suspended at a concentration of 10^7 cells/ml. The resultant *E. coli* and *S. aureus* suspension were separately spayed onto two petri dishes. The zone of inhibition was observed after all samples were placed into the petri dishes and incubated at 37°C for 24 h with growth agar.

Cell Culture

Mouse BMSCs on passages 5-6 were cultured in DMEM with low glucose supplemented with 10% FBS and 1% penicillin-streptomycin at 37°C under a 5% CO_2 atmosphere and 95% humidity. The medium was changed every 2 days. At confluence, the cells were detached with 0.25% trypsin in 1 mM ethylenediaminetetraacetic acid (EDTA), centrifuged and re-suspended in three new culture flasks for re-seeding.

Cell Viability and Morphology

The samples were placed in a culture flask and then BMSCs were seeded on the samples with a density of 10,000 cells/cm^2. After 1 day of cell culture, the samples were washed twice with PBS and transferred to a new culture flask. For Live & Dead assay, each sample was pipetted with 100 μl reagents and incubated for 30 min at room temperature in the dark. After a subsequent washing step with PBS, cell viability was examined by the use of an Olympus X51 fluorescence microscopy. For cell morphology observation, Ti-6Al-4V samples were immersed in the mixture of 2.5% glutaraldehyde and 4% paraformaldehyde solution for 4 h at 4°C, followed by washing twice with PBS for 10 mins. To dehydrate the BMSCs, all samples were alternatively treated twice with 50%, 75%, 95%, and 100% ethanol for 15 mins. Finally, the samples were coated

with platinum by using a technosyn cold cathode luminescence system and examined by a JEOL 5900 SEM.

Cell Proliferation

The MTT assay was performed to determine the level of cell proliferation. All samples were first placed in a 24 well-plate and BMSCs with a density of 10,000 cells/cm^2 were seeded on the samples. Then 1 mL DMEM medium was added to each well. After 1, 3 and 7 days of culturing, each well was added with 100 μl MTT (5 mg/ml) and incubated at 37°C for 4 h. Then the samples were transferred to a new 24-well plate and 0.5 ml dimethyl sulfoxide (DMSO) was added to dissolve the formazan crystals. After 15 mins, 200 μl DMSO was extracted to a new 96 well-plate. Finally, the absorbance was recorded at a wavelength of 570 nm.

Cell Differentiation

A quantitative real-time polymerase chain reaction (q-RT-PCR) test was performed to determine the level of representative gene expressions. BMSCs were cultured with a density of 30,000 cells/ cm^2 and collected after 2 and 7 days of osteogenic induction. The samples without osteogenic induction (day 0) were used as control. The Total ribonucleic acid (RNA) was extracted by using TRIzol in accordance with the supplier instructions. Then 1 μg RNA sample was reversely transcribed for standard cDNA synthesis. The q-RT-PCR was conducted by an SYBER Green assay (Applied Biosystems, USA). Amplification program was started with an initial denaturation at 95°C for 10 mins, followed by 40 cycles at 95°C for 15 secs and 60°C for 1 min. The five gene premiers used in this study were (form 5'-3'): ALP-F: CTC CAA AAG CTC AAC ACC AAT G, ALP-R: ATT TGT CCA TCT CCA GCC G; BSP-F: CCA CAC TTT

CCA CAC TCT CG, BSP-R: CGT CGC TTT CCT TCA CTT TTG; COL I-F: AAC AGT CGC TTC ACC TAC AG, COL I-R: AAT GTC CAA GGG AGC CAC; OPN-F: CTA CGA CCA TGA GAT TGG CAG, OPN-R: CAT GTG GCT ATA GGA TCT GGG; GAPDH-F: AGG TCG GTG TGA ACG GAT TTG, GAPDH-R: TGT AGA CCA TGT AGT TGA GGT CA. The relative expressions of genes were determined by the $2^{-\Delta\Delta Ct}$ method. GAPDH was selected as a housekeeping gene to normalize the expression levels of the target genes.

Statistical Analysis

All of the results are presented in mean ± standard deviation (SD). One-way analysis of variance (ANOVA) was used to calculate the significance level. Significant difference was considered when $p<0.05$.

■ RESULTS AND DISCUSSION

Characterization of the Alginate/Chitosan Film Construction Process

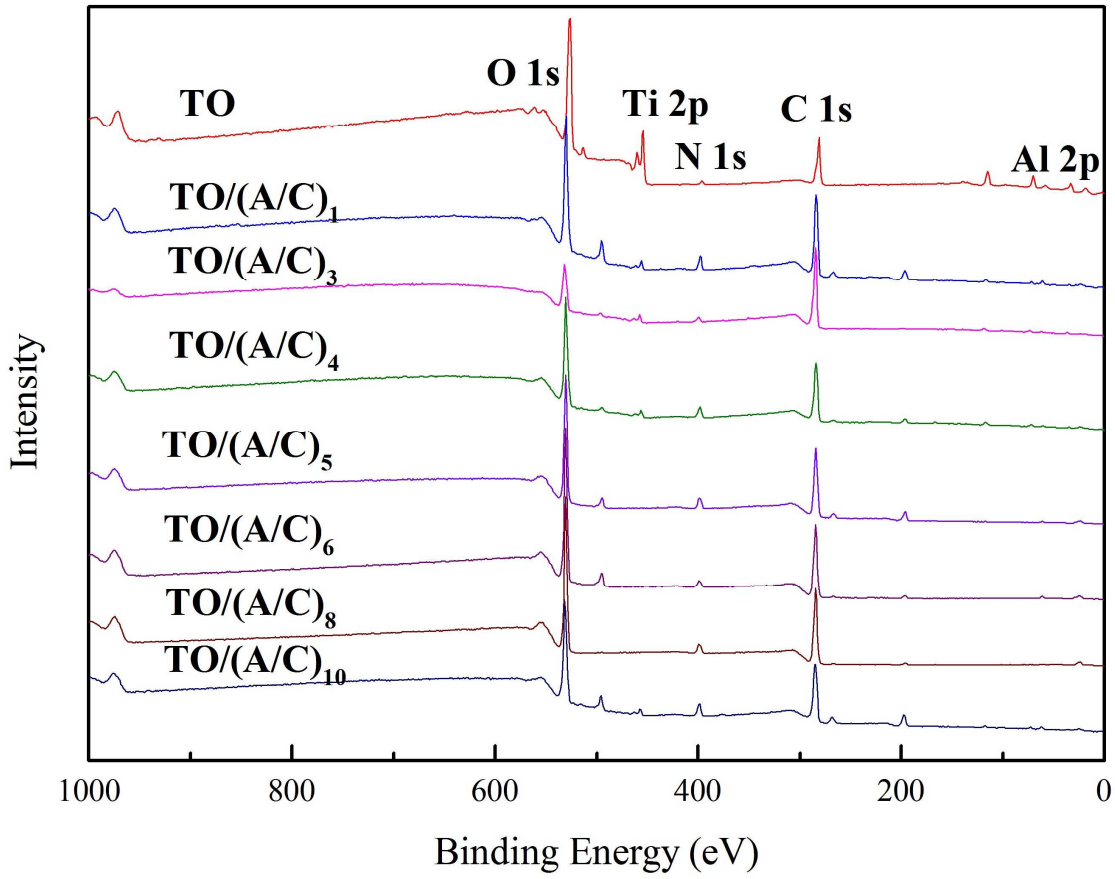

Figure 1. XPS wide scan of Ti-6Al-4V samples after different treatments (A: alginate; C: chitosan).

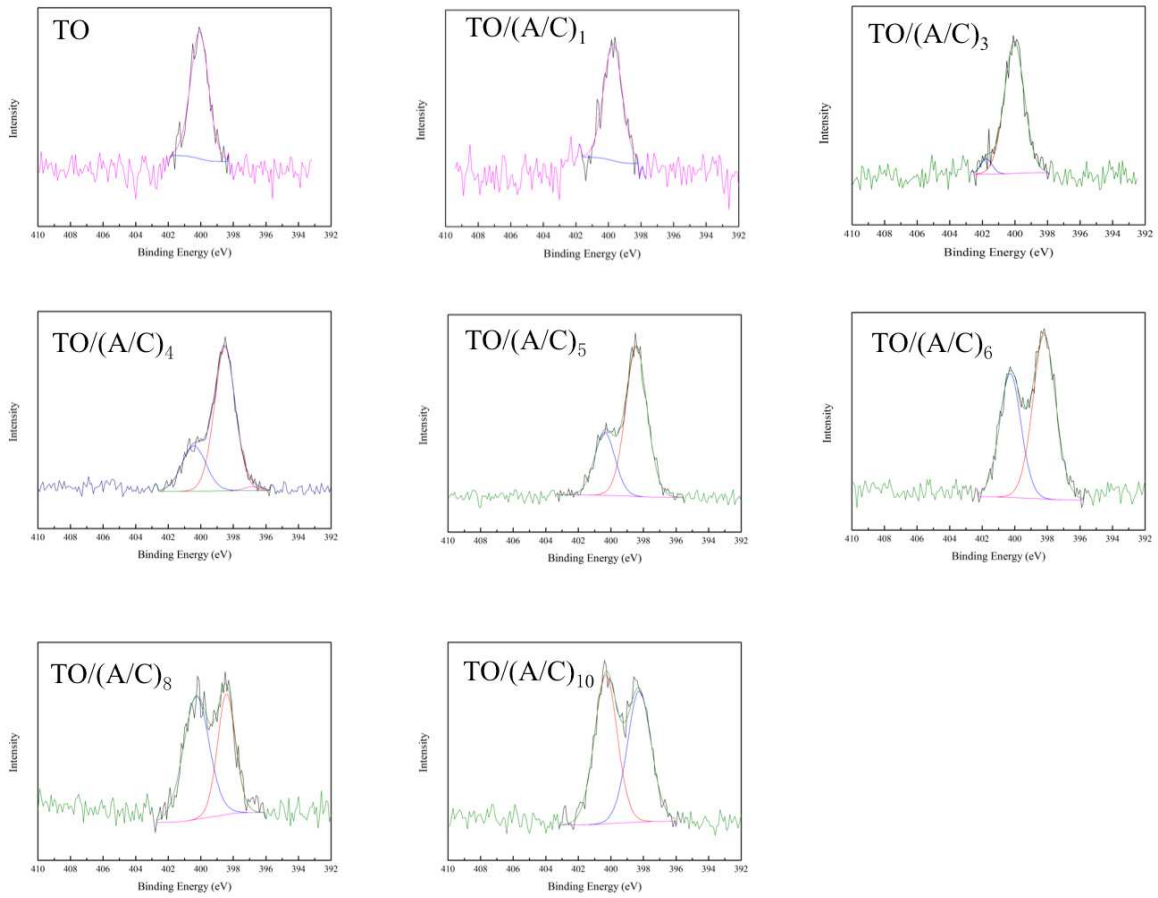

Figure 2. N 1s high resolution spectra of Ti-6Al-4V after different treatments (A: alginate; C: chitosan).

This part reports the construction process of the alginate/chitosan film on thermally oxidized Ti-6Al-4V samples. An XPS was used to investigate the surface chemistry change during the alginate/chitosan LBL assembly process. All of the spectra obtained indicate the major elements of Ti, Al, C, N and O (Figure 1). A gradual decrease in the intensity of Ti 2p and Al 2p was observed with an increasing number of alginate/chitosan pairs (data not shown). The N 1s high resolution spectra (Figure 2) demonstrate the presence of amine groups at binding energies about 398.1, with respect to the use of chitosan [21]. The amide peaks at about 401.3 eV were possibly

caused by atmospheric contamination from thermal oxidation and the partial N- deacetylation of chitin [22]. Meanwhile, the gradual increase in the intensity of amine group implies that there was a sustained deposition of chitosan onto the TO sample surface. Taken together, the X-ray spectrometry analysis confirms the layerwise deposition of alginate/chitosan onto the thermally oxidized Ti-6Al-4V surface.

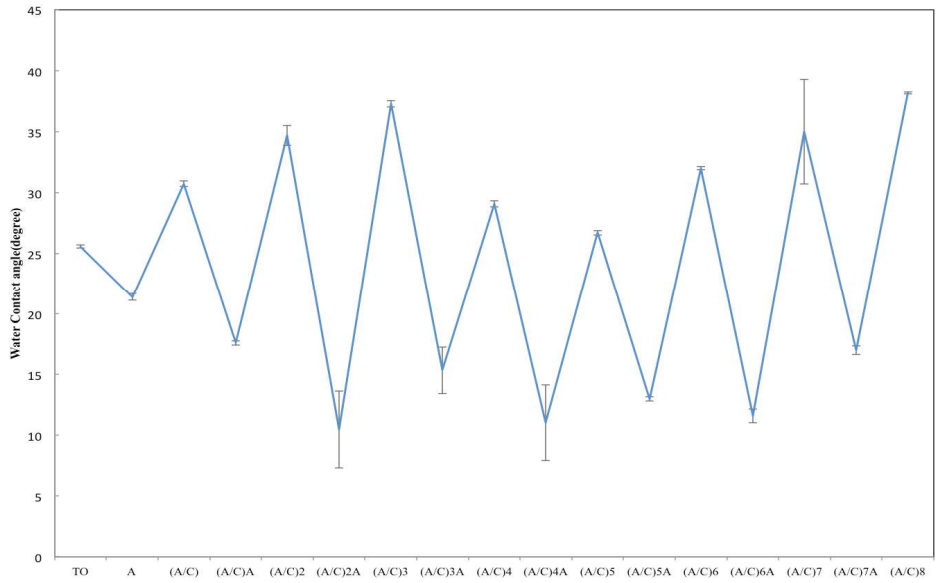

Figure 3. Water contact angle measurement during the alginate/chitosan film construction process (A: alginate; C: chitosan).

The water contact angle measurement was carried out to monitor the variation of wettability during the alginate/chitosan film construction process (Figure 2). An alternative change in the water contact angle was observed after the deposition of each alginate and chitosan single layer. This phenomenon is consistent with previous study and indicates that the TO samples were fully covered by either alginate or chitosan as the outmost layer [21]. Interestingly, J. Park et al. observed and speculated that the incomplete coverage of chitosan, poly(L-glutamic acid) and poly(L-lysine) monolayers on titanium surface is due to the 0.15 M NaCl used to dissolve these

polyelectrolytes, which results in the preferential attachment of Na^+ onto the negatively charged Ti surface [23]. However, this phenomenon is not observed in this study. It can be attributed to the PDA used prior to alginate/chitosan LBL self-assembly. The strong adhesive properties of the PDA precursor ensured the uniform deposition of the first alginate layer onto the TO sample, which in turn provided a desirable negatively charged surface for the deposition of the first chitosan layer. Accordingly, a well-organized LBL film can be formed after the alternative deposition of alginate and chitosan.

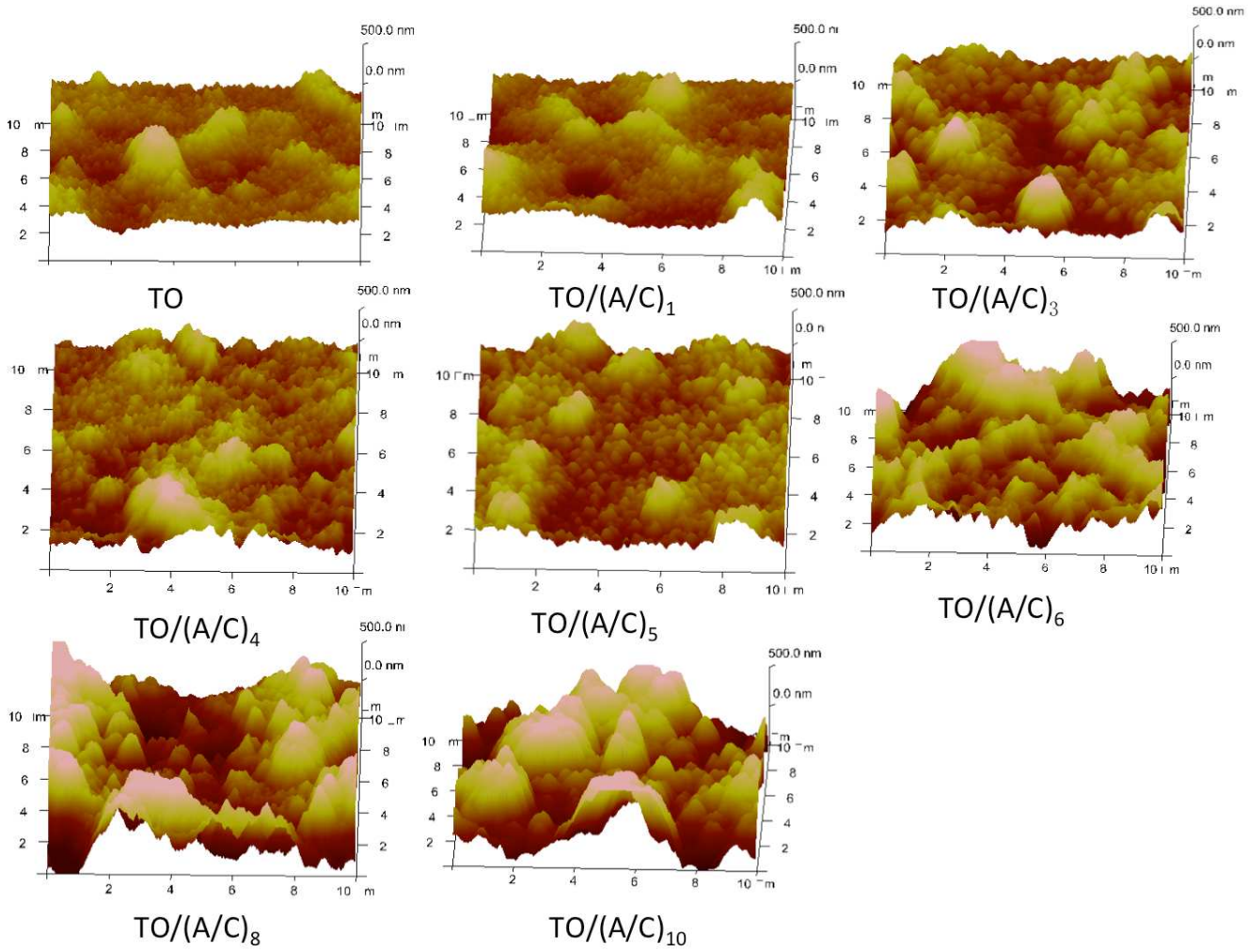

Figure 4. Surface topography change of thermally oxidized Ti-6Al-4V samples during alginate/chitosan film build-up process (A: alginate; C: chitosan. AFM scan area: 10 x 10 μm^2, z-axis height: 500 nm)

AFM was employed to monitor the surface roughness and topography changes during the alginate/chitosan film construction process. Figure 4 shows that the initial layerwise build-up did not significantly alter the surface topography produced by TO. However, the original oxide particles became larger in TO/$(A/C)_6$ to TO/$(A/C)_{10}$ samples. This phenomenon clearly indicates that the surface topography induced by TO had been altered after six pairs of alginate/chitosan LBL assembly. The topography change was further quantified by a roughness measurement. As shown in Figure 5, the average surface roughness values were stable around 80 nm in TO/(A/C) to TO/$(A/C)_5$ samples. However, the surface roughness increased to 120.03 ± 22.21 nm on TO/$(A/C)_6$ sample, and finally reached a value of 211.50 ± 22.95 nm on TO/$(A/C)_{10}$ sample. Theoretically, the spin-assisted coating would produce uniform surface layers on a flat surface, even to fabricate one single layer. However, when the surface is not flat, as shown in the current study, the result becomes more complex. It is speculated that the sudden increase of roughness was possibly caused by the rough surface, which cannot be uniformly covered by chitosan and alginate. As the increase of layer number, the surface may become rougher than conventionally dip-coated flat surfaces. Further investigation may be conducted to reveal this phenomenon. Taken together, the film made of five pairs of alginate/chitosan are preferred as an "ultrathin" film for further study because it was able to fully cover the TO sample surface, but did not significantly alter its surface roughness and topography. Further studies were, therefore, centered on the TO/$(A/C)_5$ sample.

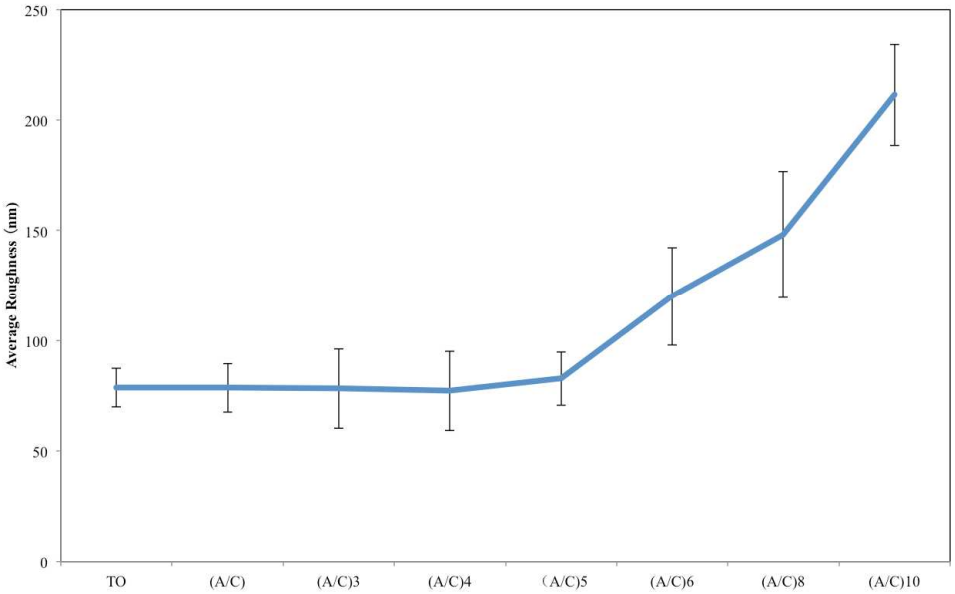

Figure 5. Surface roughness measurement of thermally oxidized Ti-6Al-4V samples with different number of alginate/chitosan pairs (A: alginate; C: chitosan)

Scanning electron microscope was used to characterize the topography of modified Ti-6Al-4V samples. The TO sample surface was consisted of numerous fine oxide particles. The TO/$(A/C)_5$ sample exhibited a comparable topography to the TO sample, but with additional nano-scale shinny particles (30 ~ 80 nm). Energy dispersive spectrometry analysis demonstrates that these shiny particles appeared to be Ag (Figure 7). Therefore, it is demonstrated that the expected hybrid thin film has been successfully fabricated on the TO sample.

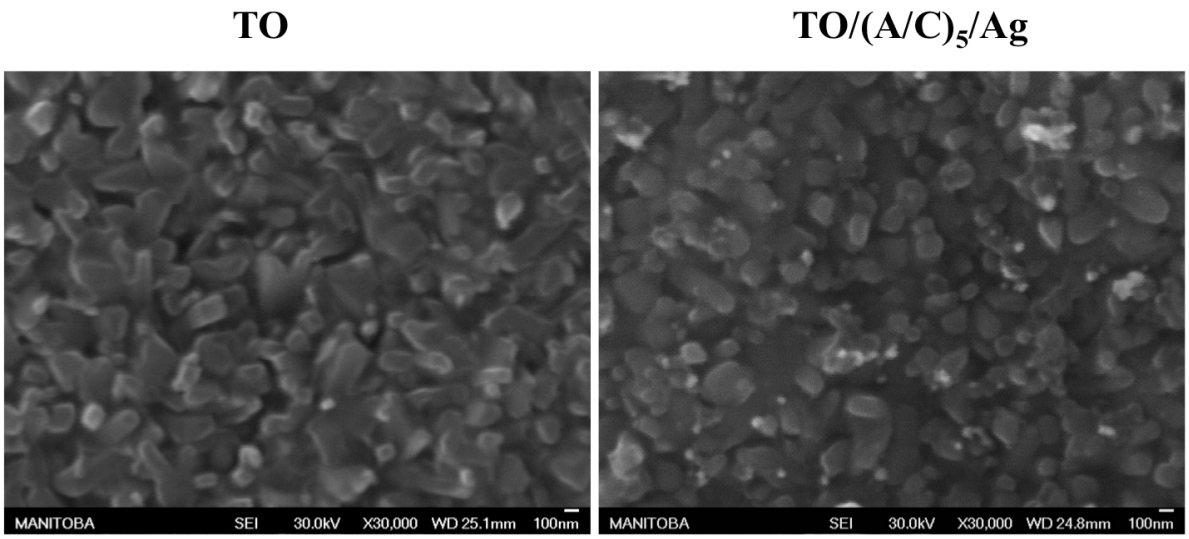

Figure 6. SEM and AFM characterizations of Ti-6Al-4V samples treated by TO and $TO/(A/C)_5/Ag$.

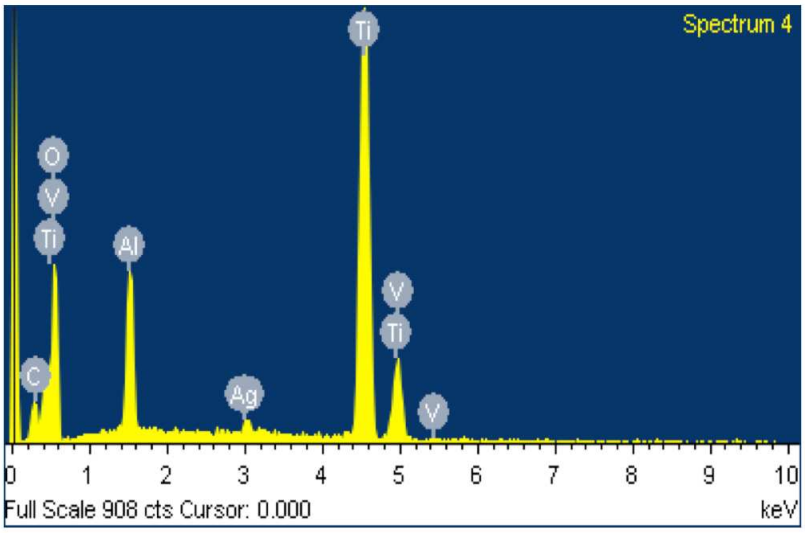

Figure 7. Energy-dispersive spectrometry analysis of the $TO/(A/C)_5/Ag$ sample.

In Vitro Evaluation

Antibacterial Test

An agar diffusion test was conducted on *E. coli* and *S. aureus* to test the antibacterial capability of different Ti-6Al-4V samples (Figure 8). No zone of inhibition against *E. coli* and *S. aureus* bacteria can be observed around the TO samples. However, the TO/$(A/C)_5$/Ag sample showed good zone of inhibition against both *E. coli* and *S. aureus* bacteria. This result indicates that the successful release of antibacterial nano-silver from the TO/$(A/C)_5$/Ag sample. In contrast, the samples without nano-silver did not exhibit any antibacterial capability.

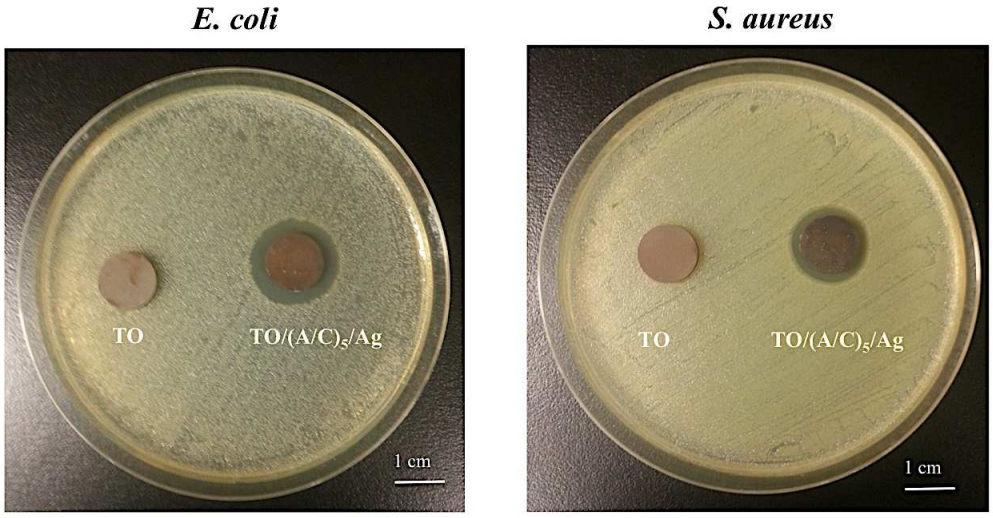

Figure 8. Zone of inhibition against E. coli and S. aureus on TO and TO/$(A/C)_5$/Ag samples.

Cell Viability and Morphology

Figure 9 shows the florescence and scanning electron microscopies images of BMSCs seeded onto different Ti-6Al-4V samples. The BMSCs exhibited higher percentage of live cells (green) than dead cells (red) on all Ti-6Al-4V samples. This result demonstrates that all the samples were safe and suitable for the growth of BMSCs. Meanwhile, BMSCs exhibited higher cell

numbers and more stretched morphologies on TO/$(A/C)_5$/Ag samples than that of TO sample. This phenomenon implies hybrid film is highly biocompatible for the initial growth and attachment of BMSCs.

Cell Proliferation

The proliferation levels of BMSCs seeded on different Ti-6Al-4V samples were studied by the MTT assay (Figure 10). BMSCs seeded on TO/$(A/C)_5$/Ag samples exhibited significantly higher levels of proliferation than those on TO samples at both 3 and 7 days of culturing ($p<0.05$). This result further indicates that the essential function of alginate/chitosan ultrathin film on BMSC proliferation. Current interpretation on the role of natural polymers in cell-implant interactions suggests that they can mimic the nature extracellular microenvironment to attract osteogenic cells from surrounding tissues to adhere onto implant surface. Then the cells start to proliferate and differentiate around wound site, thus enhancing new bone formation and bone-implant integration [24]. Our results are in good agreement with this explanation. The alginate/chitosan/nanosilver ultrathin film may partially simulate the extracellular microenvironment, which can stimulate specific cellular responses during wound healing and tissue regeneration. Therefore, BMSCs cultured on the TO/$(A/C)_5$/Ag samples can be activated in a shorter time period. In contrast, BMSCs seeded on the TO sample had an inferior performance, which implies the bio-inert natural of Ti-6Al-4V alloy. Taken together, these results indicate that the alginate/chitosan/nanosilver ultrathin film significantly enhances the proliferation of BMSC.

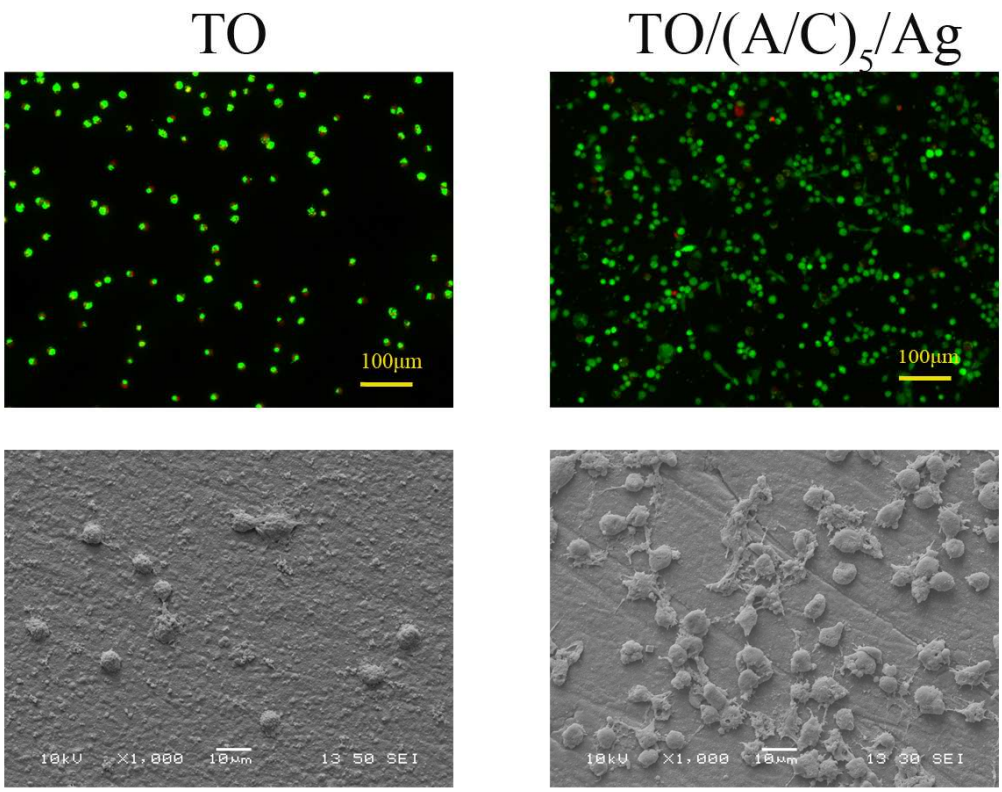

Figure 9. Fluorescence and SEM micrographs of BMSCs seeded on TO (left) and TO/$(A/C)_5$/Ag (right) samples.

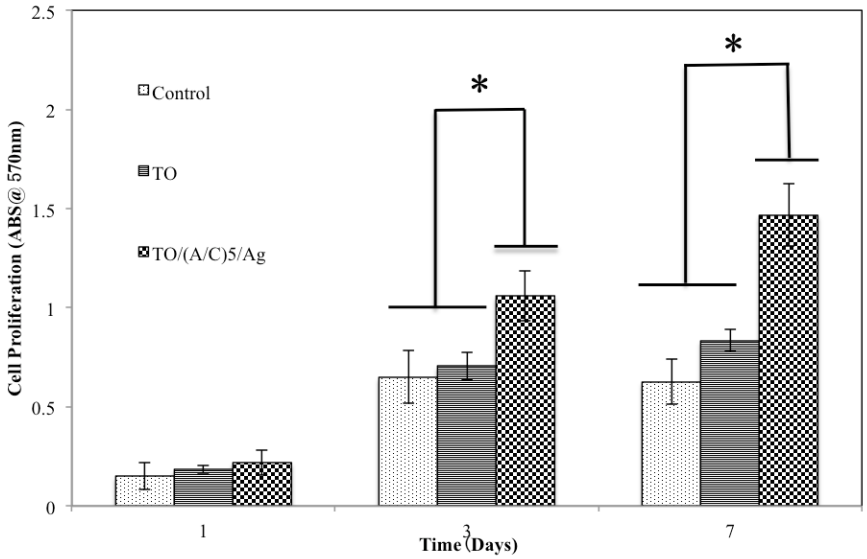

Figure 10. MTT assay. Formosan absorbance expressed as a measurement of cell proliferation from BMSCs cultured on different samples (n=4).

Cell Differentiation

The mRNA expressions of BMSC on TO/$(A/C)_5$/Ag sample were tested to investigate cell differentiation at the molecular level (Figure 11). The ALP, COL I, OPN and BSP were characterized by q-RT-PCR analysis at 2 and 7 days of BMSCs culturing. ALP, an early marker of differentiated BMSCs, was significantly increased at 7 days' culturing. COL I, the main content of bone ECM, was up-regulated at 2 days (4.29-fold) and 7 days (5.33-fold) of culturing. The other significant component of the bone ECM, BSP, was also up-regulated 1.4-fold and 4.03-fold at 2 and 7 days of culturing, respectively. However, the expression of OPN, a non-collagenous protein that binds to hydroxyapatite in ECM, decreased at 7 days of culturing (3.66-fold) when compared to that at 2 days (4.42-fold). These results indicate the positive effect of the biomimetic alginate/chitosan/nanosilver composite on BMSC differentiation. Meanwhile, the up-regulation can also be attributed to the hydroxyl and amine functional groups from chitosan,

alginate and PDA, which have been demonstrated to directly release signals to stimulate integrin binding, therefore induce a higher level of osteogenic activities [25-26]. Taken together, the hybrid film is capable of improving the ALP expression of BMSCs at early bone healing stage.

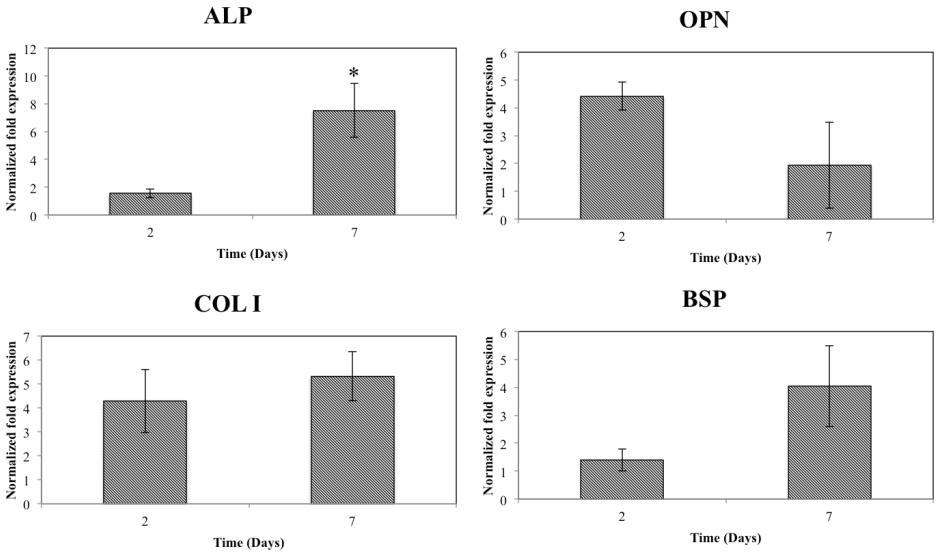

Figure 11. The relative mRNA expression of BMSCs cultured on TO/$(A/C)_5$/Ag samples (n=3).

■ Conclusion

In this study, an alginate/chitosan ultrathin film that contains nano-silver particles was successfully constructed on thermally oxidized Ti-6Al-4V surface by the use of mussel-inspired dopamine. The hybrid structure completely altered the surface chemistry of Ti-6Al-4V without deteriorating the rough surface layer induced by TO. Improvements in the BMSC viability, morphology, proliferation and demonstrated antibacterial capability have been observed *in vitro*. More importantly, BMSCs cultured onto the Ti-6Al-4V-based hybrid structure exhibited significantly higher ALP expression compared to the controls at 7 days' osteogenic induction. Overall, the combination of the surface characterizations and in *vitro* assays demonstrates that

the hybrid structure made of alginate/chitosan ultrathin film and nano-silver, developed in this work, presents functionality in enhancing the BMSC viability, proliferation and initial ALP expression, as well as antibacterial capability of thermally oxidized Ti-6Al-4V alloy.

■ AUTHOR INFORMATION

Corresponding Authors: Malcolm.Xing@umanitoba.ca and Olanrewaju.Ojo@umanitoba.ca

Author Contributions

The manuscript was written through contributions of all authors. All authors have given approval to the final version of the manuscript.

Notes

The authors declare no competing financial interest.

■ ACKNOWLEDGEMENTS

Financial supports from the NSERC of Canada, the Manitoba Health Research Council and the Manitoba Institute of Child Health are gratefully acknowledged.

■ REFERENCES

1. Saldana, L.; Vilaboa, N.; Valles, G.; Gonzalez-Cabrero, J.; Munuera, L., Osteoblast response to thermally oxidized Ti6Al4V alloy. *Journal of biomedical materials research. Part A* **2005,** *73* (1), 97-107.
2. An, S.-H.; Matsumoto, T.; Miyajima, H.; Sasaki, J.-I.; Narayanan, R.; Kim, K.-H., Surface characterization of alkali- and heat-treated Ti with or without prior acid etching. *Applied Surface Science* **2012,** *258* (10), 4377-4382.
3. Daw, A. E.; Kazi, H. A.; Colombo, J. S.; Rowe, W. G.; Williams, D. W.; Waddington, R. J.; Thomas, D. W.; Moseley, R., Differential cellular and microbial responses to nano-/micron-scale titanium surface roughness induced by hydrogen peroxide treatment. *Journal of biomaterials applications* **2013,** *28* (1), 144-160.
4. Yan, S. G.; Zhang, J.; Tu, Q. S.; Ye, J. H.; Luo, E.; Schuler, M.; Kim, M. S.; Griffin, T.; Zhao, J.; Duan, X. J.; Cochran, D. J.; Murray, D.; Yang, P. S.; Chen, J., Enhanced osseointegration of

titanium implant through the local delivery of transcription factor SATB2. *Biomaterials* **2011,** *32* (33), 8676-8683.
5. Fiedler, J.; Özdemir, B.; Bartholomä, J.; Plettl, A.; Brenner, R. E.; Ziemann, P., The effect of substrate surface nanotopography on the behavior of multipotnent mesenchymal stromal cells and osteoblasts. *Biomaterials* **2013,** *34* (35), 8851-8859.
6. Orsini, G.; Assenze, B.; Scarano, A.; Piattelli, M.; Piattelli, A., Surface analysis of machined versus sandblasted and acid-etched titanium implants. *International Journal of Oral & Maxillofacial Implants* **2000,** *15* (6), 779-784.
7. Chen, J.; Qiu, X.; Wang, L.; Zhong, W.; Kong, J.; Xing, M. M., Free‐Standing Cell Sheet Assembled with Ultrathin Extracellular Matrix as an Innovative Approach for Biomimetic Tissues. *Advanced Functional Materials* **2013,** *24* (15), 2216-2223.
8. Kumar, S.; Narayanan, T.; Raman, S.; Seshadri, S., Thermal oxidation of CP-Ti: Evaluation of characteristics and corrosion resistance as a function of treatment time. *Materials Science and Engineering: C* **2009,** *29* (6), 1942-1949.
9. Alonso, M.; Saldana, L.; Valles, G.; González-Carrasco, J. L.; Gonzalez-Cabrero, J.; Martınez, M.; Gil-Garay, E.; Munuera, L., In vitro corrosion behaviour and osteoblast response of thermally oxidised Ti6Al4V alloy. *Biomaterials* **2003,** *24* (1), 19-26.
10. Ueno, T.; Tsukimura, N.; Yamada, M.; Ogawa, T., Enhanced bone-integration capability of alkali- and heat-treated nanopolymorphic titanium in micro-to-nanoscale hierarchy. *Biomaterials* **2011,** *32* (30), 7297-7308.
11. Lutolf, M.; Hubbell, J., Synthetic biomaterials as instructive extracellular microenvironments for morphogenesis in tissue engineering. *Nature biotechnology* **2005,** *23* (1), 47-55.
12. Schierholz, J.; Beuth, J., Implant infections: a haven for opportunistic bacteria. *Journal of Hospital Infection* **2001,** *49* (2), 87-93.
13. Zhao, L.; Wang, H.; Huo, K.; Cui, L.; Zhang, W.; Ni, H.; Zhang, Y.; Wu, Z.; Chu, P. K., Antibacterial nano-structured titania coating incorporated with silver nanoparticles. *Biomaterials* **2011,** *32* (24), 5706-5716.
14. Hu, Y.; Cai, K.; Luo, Z.; Zhang, Y.; Li, L.; Lai, M.; Hou, Y.; Huang, Y.; Li, J.; Ding, X., Regulation of the differentiation of mesenchymal stem cells in vitro and osteogenesis in vivo by microenvironmental modification of titanium alloy surfaces. *Biomaterials* **2012,** *33* (13), 3515-3528.
15. Gao, W.; Feng, B.; Lu, X.; Wang, J.; Qu, S.; Weng, J., Characterization and cell behavior of titanium surfaces with PLL/DNA modification via a layer‐by‐layer technique. *Journal of Biomedical Materials Research Part A* **2012,** *100* (8), 2176-2185.
16. Jiang, T.; Zhang, Z.; Zhou, Y.; Liu, Y.; Wang, Z.; Tong, H.; Shen, X.; Wang, Y., Surface functionalization of titanium with chitosan/gelatin via electrophoretic deposition: characterization and cell behavior. *Biomacromolecules* **2010,** *11* (5), 1254-1260.
17. Martins, G. V.; Merino, E. G.; Mano, J. F.; Alves, N. M., Crosslink Effect and Albumin Adsorption onto Chitosan/Alginate Multilayered Systems: An in situ QCM‐D Study. *Macromolecular bioscience* **2010,** *10* (12), 1444-1455.
18. Cai, K.; Rechtenbach, A.; Hao, J.; Bossert, J.; Jandt, K. D., Polysaccharide-protein surface modification of titanium via a layer-by-layer technique: characterization and cell behaviour aspects. *Biomaterials* **2005,** *26* (30), 5960-5971.

19. Choi, J.; Konno, T.; Matsuno, R.; Takai, M.; Ishihara, K., Surface immobilization of biocompatible phospholipid polymer multilayered hydrogel on titanium alloy. *Colloids and Surfaces B: Biointerfaces* **2008,** *67* (2), 216-223.
20. Hu, Y.; Cai, K.; Luo, Z.; Zhang, R.; Yang, L.; Deng, L.; Jandt, K. D., Surface mediated in situ differentiation of mesenchymal stem cells on gene-functionalized titanium films fabricated by layer-by-layer technique. *Biomaterials* **2009,** *30* (21), 3626-3635.
21. Lawrie, G.; Keen, I.; Drew, B.; Chandler-Temple, A.; Rintoul, L.; Fredericks, P.; Grøndahl, L., Interactions between alginate and chitosan biopolymers characterized using FTIR and XPS. *Biomacromolecules* **2007,** *8* (8), 2533-2541.
22. Sugimoto, M.; Morimoto, M.; Sashiwa, H.; Saimoto, H.; Shigemasa, Y., Preparation and characterization of water-soluble chitin and chitosan derivatives. *Carbohydrate Polymers* **1998,** *36* (1), 49-59.
23. Park, J. H.; Schwartz, Z.; Olivares-Navarrete, R.; Boyan, B. D.; Tannenbaum, R., Enhancement of surface wettability via the modification of microtextured titanium implant surfaces with polyelectrolytes. *Langmuir : the ACS journal of surfaces and colloids* **2011,** *27* (10), 5976-5985.
24. Mendonca, G.; Mendonca, D. B.; Aragao, F. J.; Cooper, L. F., Advancing dental implant surface technology--from micron- to nanotopography. *Biomaterials* **2008,** *29* (28), 3822-3835.
25. Benoit, D. S.; Schwartz, M. P.; Durney, A. R.; Anseth, K. S., Small functional groups for controlled differentiation of hydrogel-encapsulated human mesenchymal stem cells. *Nature materials* **2008,** *7* (10), 816-823.
26. Ivirico, J.; Salmerón‐Sánchez, M.; Ribelles, J.; Pradas, M. M.; Soria, J. M.; Gomes, M. E.; Reis, R.; Mano, J., Proliferation and differentiation of goat bone marrow stromal cells in 3D scaffolds with tunable hydrophilicity. *Journal of Biomedical Materials Research Part B: Applied Biomaterials* **2009,** *91* (1), 277-286.